energies

MDPI

Article

Partial State-of-Charge Mitigation in Standalone Photovoltaic Hybrid Storage Systems

Iván Sanz-Gorrachategui [1,*], Carlos Bernal Ruiz [1], Estanis Oyarbide Usabiaga [1], Antonio Bono Nuez [1], Sergio Jesús Artal Sevil [1], Erik Garayalde Pérez [2], Iosu Aizpuru Larrañaga [2] and Jose María Canales Segade [2]

1 Departamento de Ingeniería Electrónica y Comunicaciones, Universidad de Zaragoza, C/María de Luna 1, 50018 Zaragoza, Spain; cbernal@unizar.es (C.B.R.); eoyarbid@unizar.es (E.O.U.); antoniob@unizar.es (A.B.N.); jsartal@unizar.es (S.J.A.S.)

2 Departamento de Electrónica, Mondragon Universitatea, C/Loramendi 4, 20500 Arrasate-Mondragon, Gipuzkoa, Spain; egarayalde@mondragon.edu (E.G.P.); iaizpuru@mondragon.edu (I.A.L.); jmcanales@mondragon.edu (J.M.C.S.)

* Correspondence: isgorra@unizar.es

Received: 1 October 2019; Accepted: 16 November 2019; Published: 19 November 2019

Abstract: Energy Storage in photovoltaic installations has increased in popularity in recent years due to the improvement in solar panel technology and energy storage systems. In several places where the grid is not available, in remote isolated rural locations or developing countries, isolated photovoltaic installations are one of the main options to power DC micro-grids. In these scenarios, energy storage elements are mandatory due to the natural day-night cycles and low irradiation periods. Traditionally, lead-acid batteries have been responsible for this task, due to their availability and low cost. However, the intermittent features of the solar irradiance patterns and load demand, generate multiple shallow charge–discharge cycles or high power pulses, which worsen the performance of these batteries. Some Hybrid Energy Storage Systems (HESSs) have been reported in the literature to enhance the lifetime and power capabilities of these storage elements, but they are not intended to overcome the Partial State of Charge (PSoC) issue caused by daily cycles, which has an effect on the short and mid-term performance of the system. This paper studies the impact of the already proposed HESSs on PSoC operation, establishing the optimal hybrid ratios, and implementing them in a real installation with a satisfactory outcome.

Keywords: Energy Storage Systems; Standalone Photovoltaic Systems; Hybrid Energy Storage Systems; $LiFePO_4$ batteries; Lead Acid batteries

1. Introduction

Systems that include energy harvesting, renewable sources, and energy storage are becoming more and more popular. Sometimes they are an alternative to traditional power sources but in other cases, they are the only economical way to supply energy to an isolated system (e.g., remote sites like telecom stations). However, power generation patterns do not usually match the consumption rates, so the use of intermediate energy storage elements is mandatory. Many of these have additional built-in functions such as electronic power conversion, monitoring and protections, in such a way that they are no longer just storage elements, but Energy Storage Systems (ESS).

The traditional storage technology in ESS for industrial applications has been Valve Regulated Lead Acid (VRLA) batteries [1–3]. However, Lithium-Ion technologies as $LiFePO_4$ or devices as ultracapacitors are becoming an alternative in some specific fields, depending on whether the application is an energy-oriented application or a power-oriented application [3–5]. For example, applications

such as elevators [6], need high power density so their ESS are mainly based on ultracapacitors. On the other side, applications as standalone photovoltaic systems for communication or metering stations (Figure 1), demand mid or long-term storage rather than high power peaks, so electrochemical technologies as battery packs (of the different chemistries already introduced) are best suited [1,3,7–10].

Figure 1. Standalone photovoltaic (PV) installation with metering and communication equipment.

Many applications feature complex power dynamics and cannot be strictly classified as power or energy application, but a combination of both. For this reason, the next step in the ESS evolution is to combine more than one storage element in the same system [11–15]. In this way, each type of storage element can be used at its most suitable power flow. These Hybrid Energy Storage Systems (HESSs) can be used in a wider range of applications [16–18] and offer enough flexibility to help with the inherent problems that traditional ESS possess. Thus, the main application of HESS in the literature ate the combination of power-oriented storage elements as ultracapacitors with energy- oriented storage elements as batteries [4,5,19–21]. However, they do have more uses.

HESSs in renewable energy applications have been studied in long-term techno-economic analysis, with simple system architectures [14,15,20] and multiple strategies and energy sources. For the specific case of photovoltaic (PV) installations, researches have led to a patent including the system architecture and a simple energy management strategy [22]. The hypothesis is that a cycle-oriented chemistry (as $LiFePO_4$) aids the conventional storage element (VRLA), improving overall long-term performance. The conclusions are positive, with the hybrid system performing better than the regular one in terms of battery aging and service life extension. However, standalone photovoltaic installations suffer from specific issues derived from repeated solar cycles known as Partial State of Charge (PSoC) [23–27]. This effect worsens the short and mid-term performance by decreasing the available battery capacity even when the battery is at the beginning of its life. A HESS can help the system to overcome this effect too.

This paper analyzes the short and mid-term benefits of using state of the art HESS architectures in these installations, similar to those proposed in [22,28] (Figure 2), but quantifying the impact of the system under PSoC operation. The storage technologies analyzed are VRLA and $LiFePO_4$ batteries, and the goal is to determine the best hybrid design that further enhance the mid-term performance.

Several HESS sizes with different hybrid technology percentages have been simulated under real consumption and generation patterns using $LiFePO_4$ and VRLA OPzS battery models, and the best design regions have been established. The concept has been validated in field application, showing better performance than the non-hybrid case and enhancing the operation under PSoC conditions up to 35%.

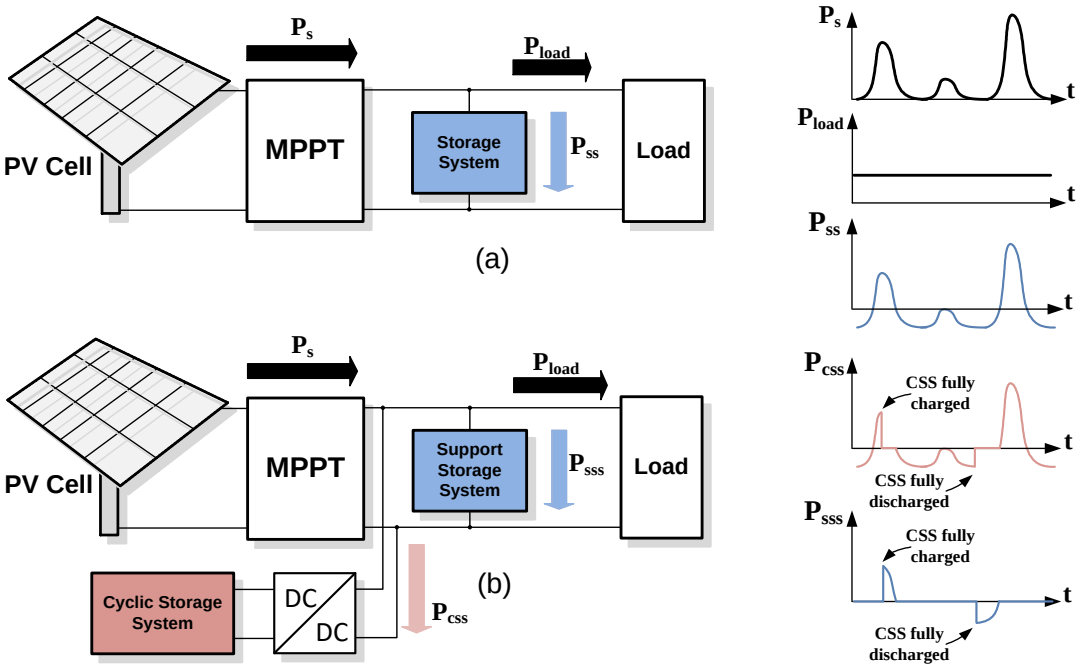

Figure 2. Conventional ESS scheme (**a**), Hybrid ESS scheme (**b**).

The paper is organized as follows: Section 2 describes the standalone photovoltaic systems and the key issues they suffer from, specifically PSoC. Section 3 reviews the HESS sizing methods, explaining some key parameters in these specific applications. Section 4 introduces the analysis that has been carried out to find the optimum HESS design regions for these installations, along with battery models and control strategies. Section 5 shows the experimental test bench and results that have been obtained, while the conclusions are collected in Section 6.

2. Specific Issues in Standalone Photovoltaic Systems

Standalone PV systems feature irregular generation profiles, which depend on sun irradiation, location, climate etc. Broadly speaking, they show two main generation/consumption dynamics: day–night cycles, and cloudy periods (days or weeks). Thus, they need energy storage modules, which have been traditionally based on Valve Regulated Lead-Acid (VRLA) batteries. In this application, one of the key issues these systems suffer from are incomplete charge/discharge processes, which lead to Partial State of Charge (PSoC) [23–27]. There are other second order issues, such as temperature, which also worsen the performance of these installations.

2.1. Incomplete Charge Process

Continuous and shallow charge–discharge cycles drive the conventional ESSs into an intermediate state of charge, also known as PSoC. To depict this effect, a typical controlled charge process, Figure 3a, is compared with an off-grid PV charge process, is shown in Figure 3b. In Figure 3a, the hypothesis is that a 0.01 C charging current is permanently available. As it can be appreciated, the battery Open Circuit Voltage (V_{ocv}) rises slower than the battery voltage (V_{batt}). During the current regulation phase, also called bulk stage, the battery absorbs the maximum available power in the system. When the float voltage is reached, the battery charger changes to the voltage regulation phase, and the battery current decreases following a path determined by its impedance model, the open circuit voltage V_{ocv} and the battery voltage V_{batt}. The battery remains in this low-power state until it is fully charged. According to VRLA manufacturers, this technology takes 72 h (3 days) in the voltage regulation phase to get to the full-charge state [29].

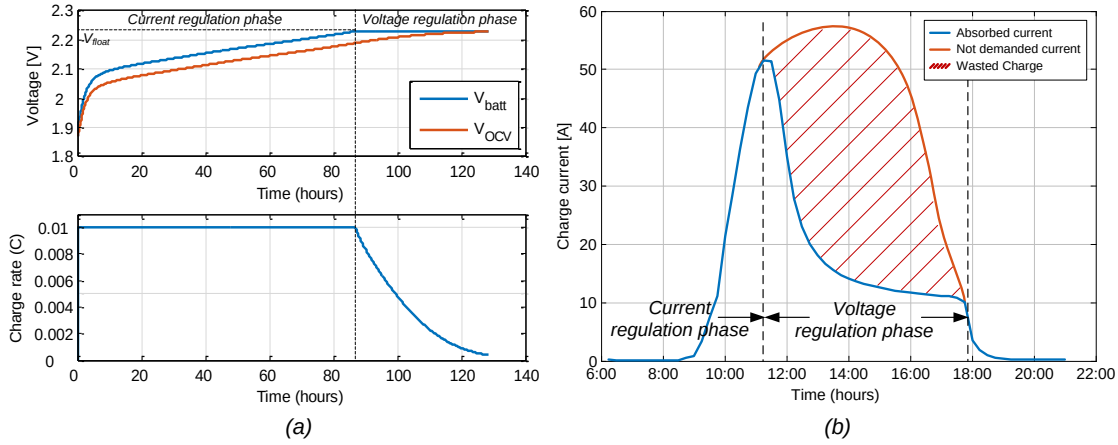

Figure 3. Different stages during charge. Controlled charge process (**a**), PV charge process (**b**).

In a standalone PV system, batteries are charged during the day and discharged during the night. On a regular day, the generation power reaches its peak value at noon, when the current flowing to the battery is maximum. This high current combined with the series impedance increases the battery voltage and the floating voltage is reached quickly. At this moment, the solar controller switches to voltage control mode, and the current begins to decrease. Paradoxically, when the available solar resource is maximum, the power generation rate decreases. As irradiation hours are limited, a single battery cannot be in the floating stage during the required 72 h. Concisely, the system wastes energy on the generation peak and additionally, the full charge state is, by definition, unreachable. All the standalone photovoltaic systems (e.g., telecom base stations, weather stations, or ditch control installations) suffer from this issue.

In the medium term (weeks), these incomplete charge processes lead the battery into a PSoC, see Figure 4. This example is based on one of the best Spanish irradiation environments (Zaragoza), where the actual State-of-Charge (SoC) is stabilized around 65% after operating for two months. This value depends on the generation pattern and particularly, on the series impedance and the SoC/V_{ocv} curve of the chemistry. In order to mitigate this issue, solar chargers use different float stages, but this strategy does not solve this problem completely and accelerates battery aging.

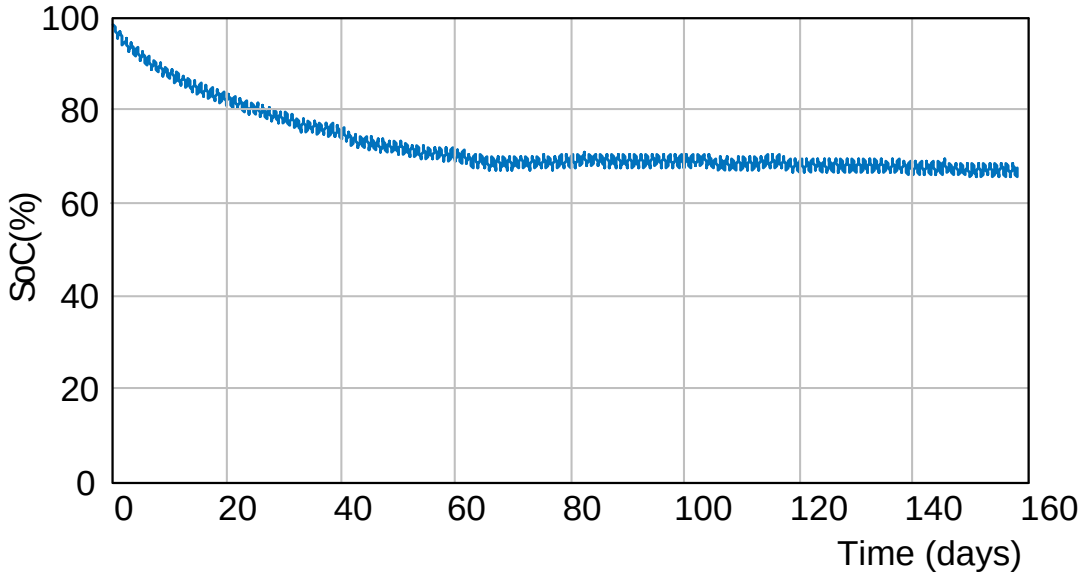

Figure 4. SoC transient evolution due to the incomplete charge effect.

2.2. Temperature Effect

Standalone installations also suffer from temperature variations. In a cost-effective installation (without temperature regulation) battery packs suffer from temperature drifts in the night–day cycle and, more importantly, in the winter–summer cycle. These temperature variations have a great impact on certain battery technologies, and in different ways. For example, in cold operation a VRLA battery capacity can shrink down to 60% of the original, whereas in hot environments the capacity can grow up to 10% (though hot operation degrades the battery faster) [29,30]. Other technologies as $LiFePO_4$ are more resilient to capacity changes due to temperature but they should not operate below 0 °C, or above 60 °C [31].

This paper focuses on the study of HESS in order to mitigate the problems derived from partial charging processes in off-grid PV installations. The study of HESS as a solution for temperature-derived issues could be also of interest but it falls out of the scope of this work.

3. HESS in Standalone PV Applications

As stated before, storage systems in PV Off-Grid applications have been traditionally based in stationary battery chemistries as VRLA [1,3]. Other storage technologies, as Lithium-Ion based chemistries, feature smaller series impedance and flatter and a more non-linear V_{OCV} curve, which makes them enter the float stage later than VRLA batteries, and with a higher SoC. Thus, these new technologies can perform better by overcoming PSoC. However, it does not make sense to invest a high amount of economic resources in new full-Lithium-Ion installations nowadays, due to the continuous decrease in the cost of Lithium-based technologies, still far from a steady state. Thus, hybrid battery packs may be considered to achieve a good performance vs. cost tradeoff. Both technologies, Lithium-Ion and VRLA, can be combined into a HESS, assigning to each technology the most suitable function. The former is less susceptible to the PSoC problem and therefore it will maximize energy storage during day/night cycle, whereas the latter will act as charge reservoir and will be in a quasi-permanent float state. This way the maximum available charge is guaranteed in the system when cloudy or misty periods arrive. Furthermore, the HESS includes some additional features that enhance the performance of the system, as storage redundancy.

HESSs have been proposed for similar applications [9,15,17,22,28], where a small pack of $LiFePO_4$ cells is combined with a bulk pack of VRLA technology. These studies mainly address lifetime extension and absorption of the battery packs. By contrast, we will analyze the impact of this HESS in terms of PSoC mitigation and study the key sizing parameters and design region that further relieve this

effect. For this reason, we will also consider $LiFePO_4$ as the Lithium-Ion technology to be used [32]. Furthermore, the flatter open circuit voltage curve and lower cost (compared to other Lithium-Ion technologies) make it a perfect candidate. Its main drawback, a lower energy density, is not critical in this application since neither compactness nor low weight are required.

3.1. System Parameters

The sizing of regular ESS used in standalone photovoltaic applications has been studied in [33–35], where different methods are presented. Khatib et al. [33] describe a review of different parameters (level of autonomy, total cycle life cost, loss of load probability etc.) and sizing methods in conventional off-grid photovoltaic installations, and the authors analyze the influence on conventional energy storage systems. The design parameters can be summarized in two parts: production capabilities and storage capacity. When designing a system with an HESS, some other factors appear, related to each storage element and the hybrid percentage.

Some of the key parameters of the proposed HESS are related to the PV installation:

- P_{gen} [W]: Peak PV power generation, i.e., the nominal PV cell power, provided by the manufacturer.
- P_{cons} [W]: Power consumption in the site. In this application, we assume it to be constant and known.
- *GR*: Generation Ratio. A dimensionless parameter that relates the PV installed peak power and the power consumption, see Equation (1). This value is closely linked to the average generation hours that the location of the installation performs. In this paper, this value remains fixed as the focus is on the storage system, but its impact will be analyzed in future research.

$$GR \triangleq \frac{P_{gen_{pk}}[W]}{P_{cons}[W]} \tag{1}$$

Other parameters related to the HESS design are the following:

- E_{VRLA} [Wh]: Installed energy in VRLA technology.
- $E_{LiFePO4}$ [Wh]: Installed energy in $LiFePO_4$ technology.
- E_{tot} [Wh]: Maximum amount of energy that can be stored in the system, see Equation (2).

$$E_{tot} \triangleq E_{VRLA} + E_{LiFePO4} \tag{2}$$

- E_{stored} [Wh]: Total amount of energy that is stored in the system at a given time.
- *A* [h]: Maximum autonomy of the system. It is directly related to *Etot* and *Pcons*. This parameter makes possible to compare different installation sizes (in absolute power) with similar *GR* and *A* parameters.

$$A[h] \triangleq \frac{E_{tot}[W]}{P_{cons}[W]} \tag{3}$$

- P_{conv} [W]: Maximum power that can flow through the converter. It depends on the specific converter, design and topology.
- F_{hy}: Hybrid factor. Defined as in Equation (4). A low F_{hy} assumes that most of the storage is based on VRLA technology, while a high F_{hy} means a higher presence of $LiFePO_4$ batteries.

$$F_{hy} \triangleq \frac{E_{LiFePO4}}{E_{tot}} \tag{4}$$

- State of Energy (%): In a HESS, each battery can have different nominal voltages, so talking in terms of charge and SoC has less sense than doing it in terms of energy. For this reason, State of Energy (SoE) is used as metric (5). This can also be defined for a simple ESS.

$$SoE(\%) \triangleq \frac{E_{stored}}{E_{tot}} x100 \tag{5}$$

3.2. System Architecture

A HESS requires the exchange of power between different energy storage devices, so a power-electronics based DC/DC converter is required. Besides the storage technologies, there is an important field of study in the system architecture (how to arrange the storage elements, loads, and power converters). For this purpose, different categories of HESS have been proposed in the state of the art [36]. Most of the proposals [11,16,36,37] are generally included in one of these two types of architectures:

- Cascaded block architectures, semi-active [36]. See Figure 5a.
- Common DC bus architectures, active [36]. See Figure 5b.

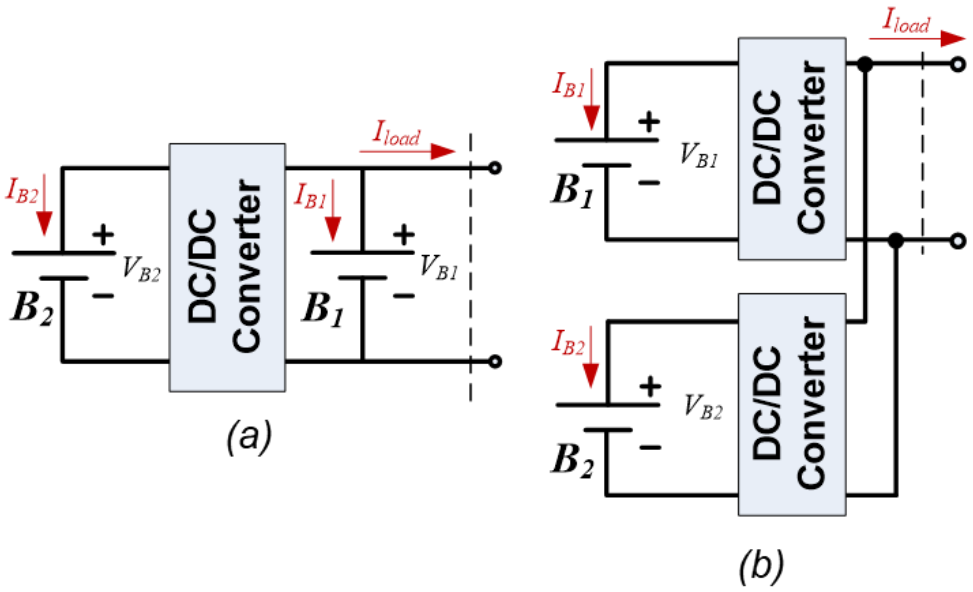

Figure 5. Cascaded architecture (**a**). Common DC bus architecture (**b**).

To analyze the benefits of the HESS, the semi-active option, Figure 5a, is selected. This system architecture has some benefits over the common DC bus architectures. It uses less converters and it is a Plug&Play concept, which can be connected in parallel to an already existent ESS. Furthermore, some applications as telecom base stations must always have a battery in parallel with the load as a security measure, so the common DC bus option would not be allowed. The only restriction the cascaded architecture has is that the load needs to be able to operate at B1 voltage, and in some cases, the load would need to have its own unidirectional input DC/DC converter.

4. HESS Simulation

To find the optimum design regions for HESS applied to our problem, multiple different designs are simulated. In these simulations, Autonomy and F_{hy} are varied. The results are compared against one system with a conventional ESS based on a single VRLA battery pack. The models and control strategies are introduced in the following sections.

4.1. Battery Model

Battery models, their parameters and estimators have been widely studied [2,38–43] in many different applications. A simple but effective way to model a battery is to consider its Equivalent Circuit Model (ECM), which is able to replicate PSoC conditions [24,42,43]. Some of these models include a non-linear capacitor whose capacitance varies along its voltage range, in series with an impedance (Figure 6a). A widely assumed model for the series impedance consists of a series resistor and one (or more) parallel RC tanks. Some parameters are defined here:

- C_{bulk}: non-linear bulk capacitance that models the battery storage capability. It depends on the battery internal voltage *Vocv*.
- R_s, R_p, C_p: parameters of the series impedance, considering a One Time-Constant (OTC) model.
- V_{ocv}: Open Circuit Voltage of the battery. It is related to the internal electro-chemical state, and it can only be measured when the relaxation process has finished after a period of zero current ($Vcp = 0$ V).
- V_{batt}: voltage measured at the battery terminals, whether there is current flowing or not.
- I_{batt}: current that flows into the battery terminals.

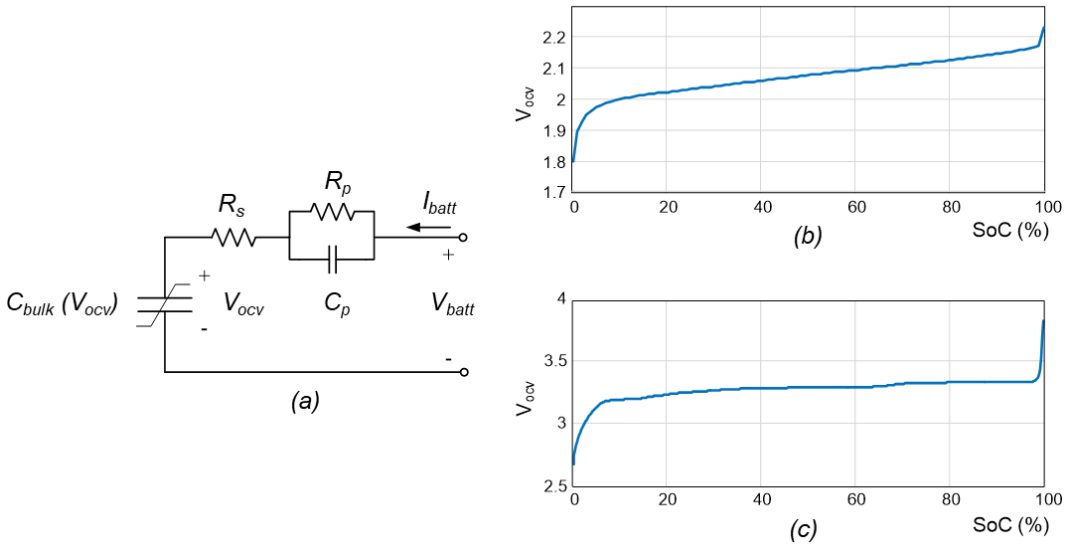

Figure 6. OTC Non-linear capacitance model (**a**), SoC–Vocv curve for VRLA technology (**b**), SoC–Vocv curve for $LiFePO_4$ battery (**c**).

This model does not consider some second order effects such as intra-cycle temperature drifts, auto- discharge or aging processes, as the focus of the paper is to determine how the hybrid system and the control strategy enhance the short and mid-term performance of the system. Nevertheless, it is able to replicate one of the key underperforming scenario in PV installations in the short and mid- term timespan, which is the incomplete charging process, since it depends mainly on the series impedance (R_s, R R_p, C_p) and on the battery chemistry (SoC–V_{ocv} characteristic curve). The model equations are collected in (6).

$$\begin{cases} \frac{dV_{cp}}{dt} = \frac{1}{C_p}\left(I_{batt} - \frac{V_{cp}}{R_p}\right) \\ \\ \frac{dV_{ocv}}{dt} = \frac{I_{batt}}{C_{bulk}(V_{ocv})} \end{cases} \quad (6)$$

where C_{bulk} is defined as differential or small signal capacitance and depends on V_{ocv} and thus is modeled by a voltage-controlled capacitor [44–48]. It can be extracted from the SoC–V_{ocv} curve of each chemistry (Figure 6b,c) as in (7). Here Q is the stored charge in the battery, and it is related

to SoC through the rated capacity of the battery. C_{bulk} is not constant and varies depending on the existing V_{ocv}.

$$C_{bulk}(V_{ocv}) \triangleq \frac{\delta Q(V_{ocv})}{\delta V_{ocv}} = C_{rated} \cdot \frac{\delta SoC(V_{ocv})}{\delta V_{ocv}} \quad (7)$$

4.2. Simulation Approach

In order to characterize the advantages of HESS, a basic HESS (Figure 7a) is compared to a simple ESS with only one battery pack, see Figure 7b. Both systems will offer the same overall storage capacity and will be connected to the same current generation (I_{gen}) and load current (I_{load}) patterns. Several HESS designs are studied by variating some relevant system parameters, as the hybrid factor F_{hy} or the autonomy A. The comparison is then based on some figures of merit, which are introduced in the following sections.

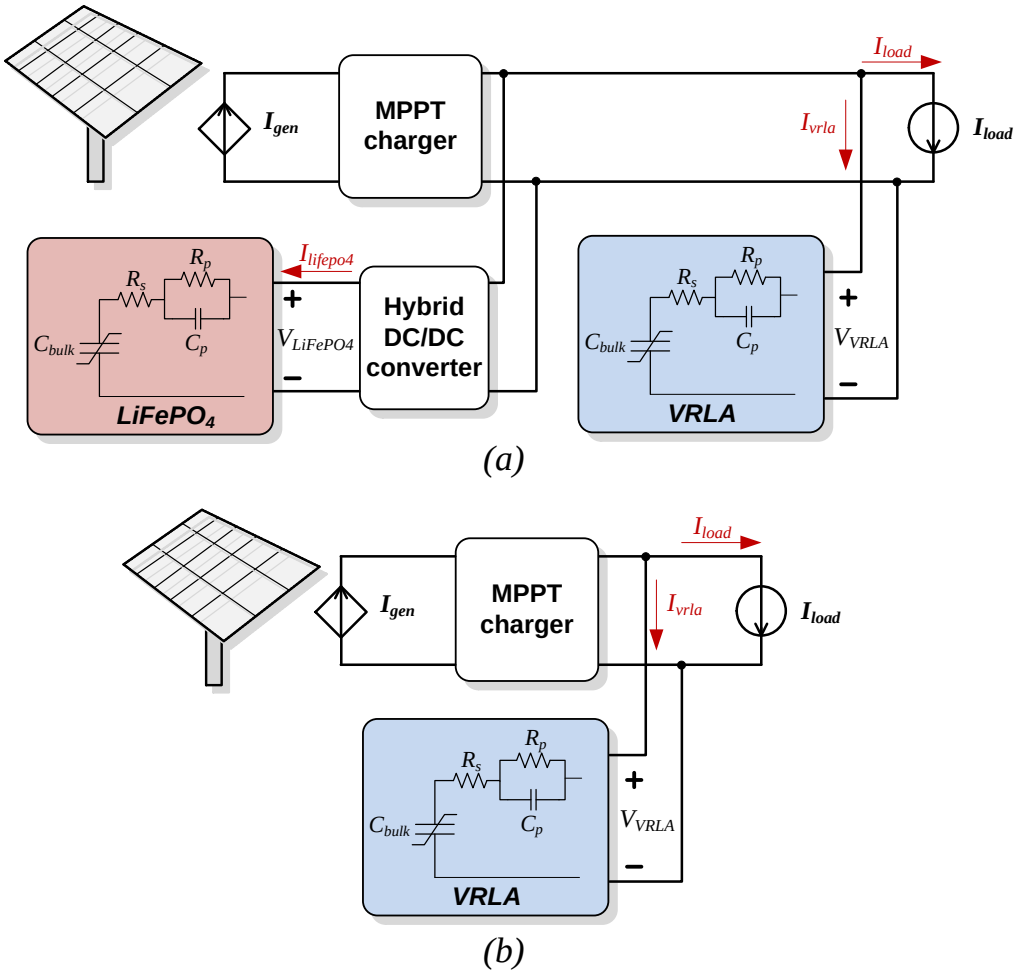

Figure 7. Circuital simulation scheme.

Data from a real installation was used to establish the current consumption and generation waveforms. The installation has a DC consumption of 3 A at 24 V, so P_{cons} = 72 W, and it has 700 W_{PK} of P_{gen} installed, so GR = 9.72. Each simulation case replicates PV irradiation waveforms measured during years 2013, 2014, 2015, and 2016, sampled each 15 min. Although the goal is not to evaluate the long-term performance and lifetime improvement, several years were evaluated to obtain good averaged SoE metrics, less dependent on particularly good or bad years in terms of irradiance.

An Energy Management Strategy (EMS) is needed in order to obtain simulation results. For this purpose, a simple priority EMS was implemented in the simulator, see Figure 8 The selected EMS gives

full priority to the charge and discharge processes in the $LiFePO_4$ battery, relegating the VRLA battery to an emergency role. This technology assignation fits with the features of each chemistry type [11], resulting in quick energy absorption and faster recovery during low irradiation days thanks to the $LiFePO_4$ battery, and ensuring a completely full VRLA battery when it is needed. This strategy differs from the one presented in Ref. [22], since their priority was charging the VRLA battery. However, that strategy does not benefit from the cycling capabilities of the Lithium-Ion element, and was evolved in refs. [28,36]. In this application, the EMS is implemented through the DC/DC hybrid converter, while the conventional Maximum Power Point Tracking (MPPT) charger only manages the float process in the conventional battery. Deeper research in EMS is a promising field of study but it is out of the scope of this paper.

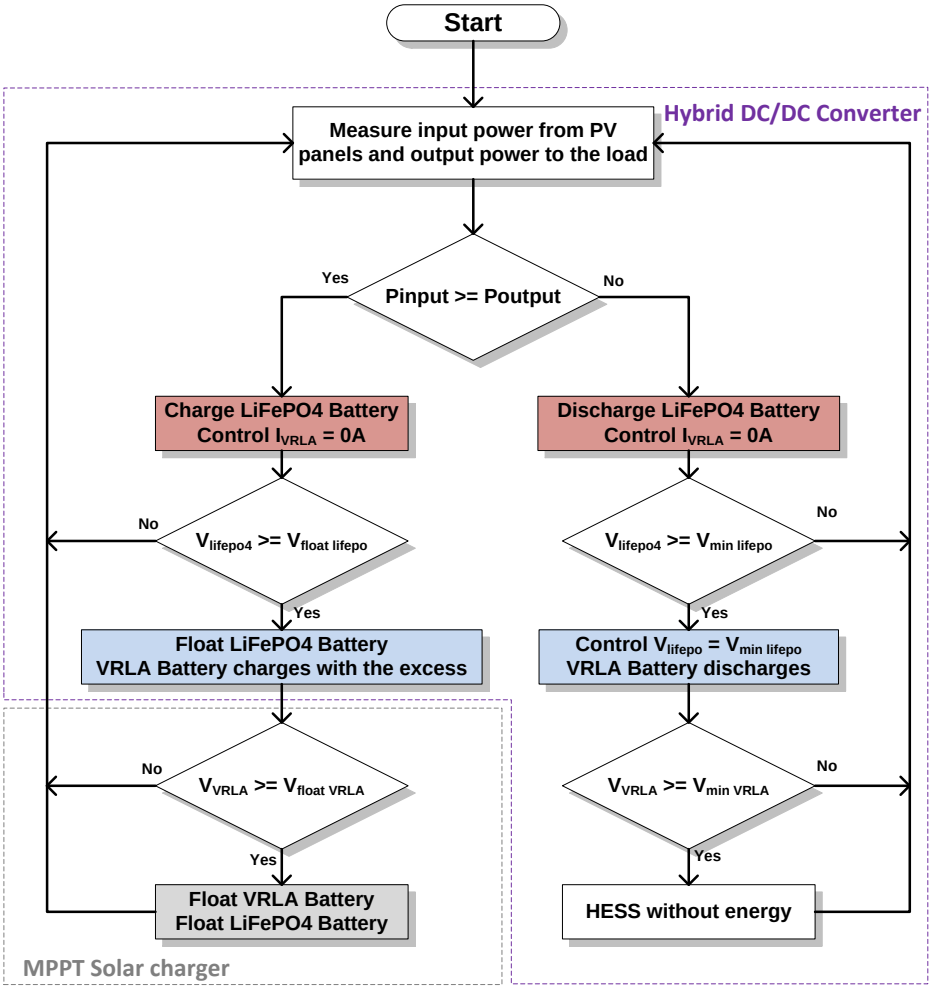

Figure 8. Simple priority EMS.

Each battery technology was tested using the procedure described in Ref. [41]. The ECM parameters were characterized from these tests, and their average values are collected in Table 1. Simulations take into account the actual efficiency curve measured from a typical bidirectional DC/DC converter.

Table 1. ECM parameters for each chemistry.

Battery	Parameter	Value	Units
VRLA	*Rs*	*180*	*mΩ*
	Rp	*50*	*mΩ*
	Cp	*9.4 e4*	*F*
$LiFePO_4$	*Rs*	*50*	*mΩ*
	Rp	*50*	*mΩ*
	Cp	*1.8 e4*	*F*

In order to determine the optimal HESS size and its benefits, Autonomy and F_{hy} are swept. After the simulation, some figures of merit are processed:

- Steady SoE improvement: the additional steady energy that the HESS maintains compared to the conventional ESS (expressed in percentage).
- Number of system failures (if any). Failures are caused by under-voltage situations on the VRLA battery.
- Loss of Load Probability (LOLP). Fraction of time the system remains without energy, and therefore it cannot provide energy to the load.
- Recovery improvement: the additional energy that the HESS harvests in a sunny period just after a system failure or low irradiation period, compared to the energy that the conventional ESS harvests.

The Figure 9 shows an example of several simulation months for one of the simulated design points. The evolution of the SoC of each battery in both systems can be appreciated.

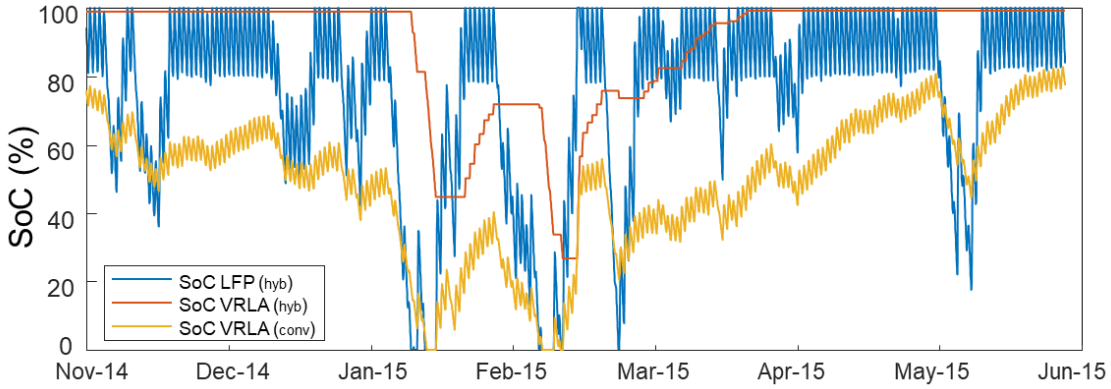

Figure 9. Simulation example for several months with one design point.

4.3. Simulation Results

The simulation results are shown in the next figures. In Figure 10a, the steady SoE improvement for a sample case is depicted, while Figure 10b shows this metric for the whole design region. As displayed, for each autonomy value the optimal F_{hy} that ensures maximum energy absorption from the PV source is located around 20%–35%. Beyond this value, the SoE increase does not grow further (despite the fact that the HESS gains in chemistry quality and thus, becomes more expensive). This is a very interesting result, as it establishes that a Hybrid Lead-Acid + $LiFePO_4$ system performs better than a single battery $LiFePO_4$ system, which has a much higher cost. It can be explained as follows: in a single battery system, both chemistries, Lead-Acid and $LiFePO_4$, suffer from PSoC though it has less impact in the $LiFePO_4$ battery. In a HESS with a high priority EMS, only the high priority battery ($LiFePO_4$) suffers PSoC. With low F_{hy}, this battery is small, so the incomplete charge overall losses are small, and the gains of having the Lead-Acid battery in a fully charge state are more evident. When F_{hy} grows, the high priority battery has higher capacity, and thus the overall impact of the incomplete charge effect is

bigger. While there is still an important benefit over conventional ESS, the benefits of HESS become less evident. This will be further discussed in the conclusions section.

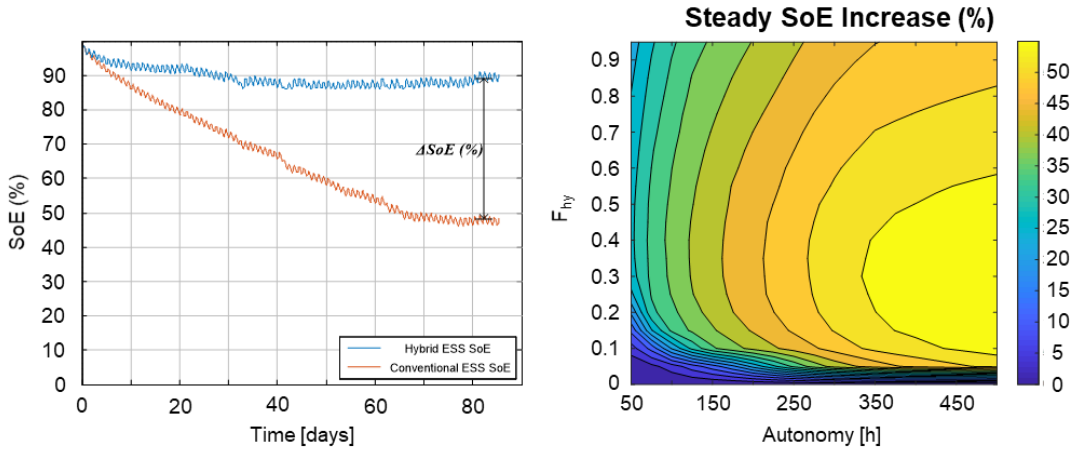

Figure 10. Sample Steady SoC increase (**a**), Steady SoE increase map (**b**).

As an example, if F_{hy} = 20% is selected, the number of energy shortage events per year is depicted in Figure 11. For the specific irradiation conditions and the P_{gen} and P_{cons} values that are being simulated, there is a minimum autonomy value of 225 h which ensures a failure-less operation and allows SoE improvement. Increasing the autonomy further than this value does not improve the benefits of the HESS performance. Compared with the conventional ESS, the HESS guarantees a failure-less operation with half of the total autonomy size, which for the same consumption conditions means half of the battery capacity.

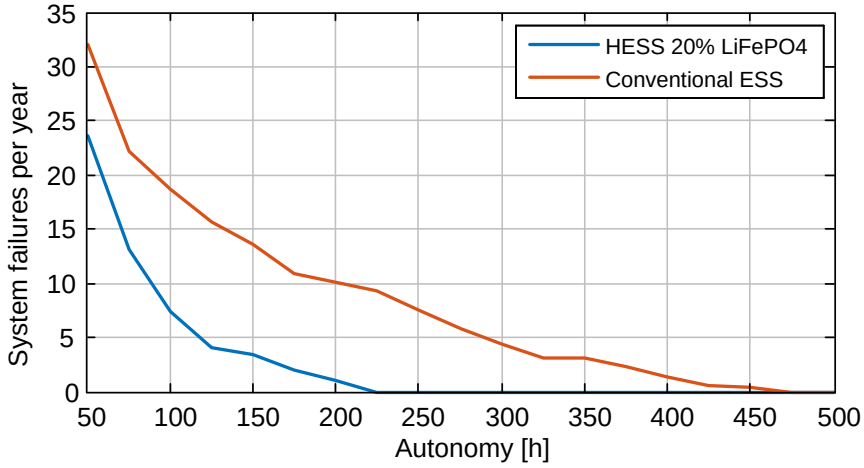

Figure 11. System failures per year (F_{hy} = 20%).

By contrast, we can fix the autonomy of the system and analyze how the performance of the installation evolves when increasing the percentage of lithium-ion technology. Figure 12 shows an example, where A has been fixed to 150 h. Here it can be appreciated how LOLP decreases when the amount of $LiFePO_4$ grows, while making HESS more expensive.

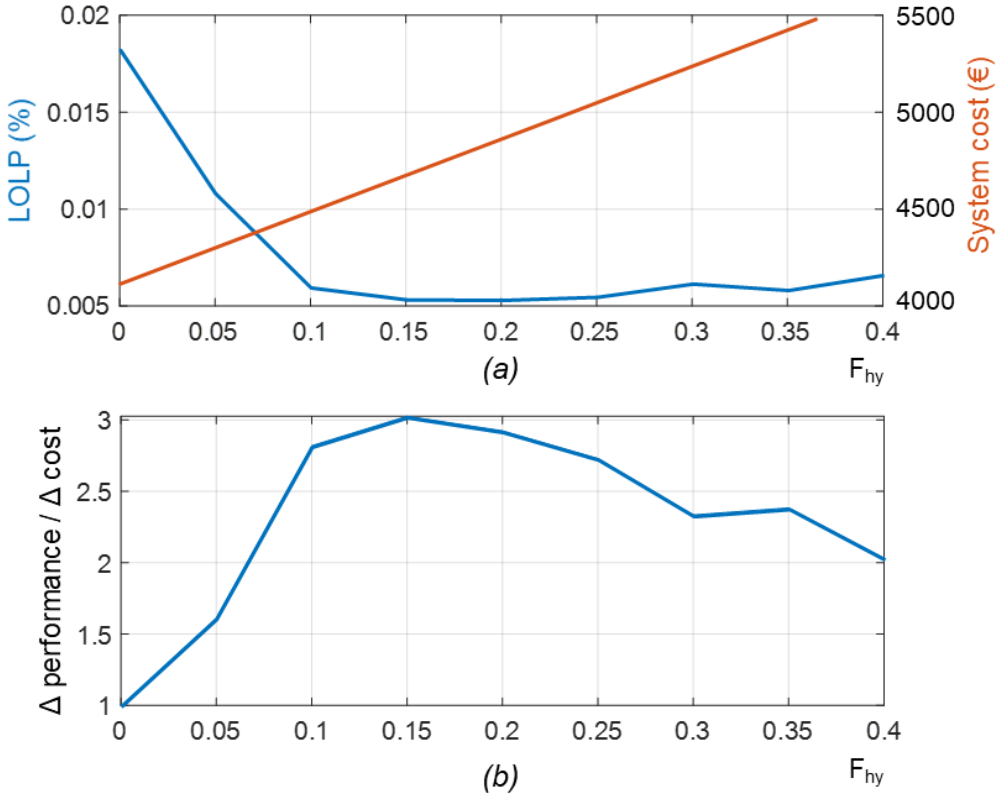

Figure 12. Different metrics for A = 150 h. LOLP and system cost (**a**), Performance increase vs cost increase with respect to the non-hybrid case (**b**).

Defining the performance as the inverse of the LOLP, Figure 12 shows the relative increase in performance vs the relative increase in cost for every F_{hy} compared to the non-hybrid case. For this figure of merit, the optimum is found around 15%, a little lower that the case SoE increase. For this simulation, the prices considered were 0.2 €/Wh for the VRLA technology and 0.5 €/Wh for $LiFePO_4$ technology. The price of the solar panels was considered constant in every case (2 €/W).

As the last figure of merit, Figure 13a shows the recovery capabilities of each system after a very low irradiation period, where the system suffered from energy disruption. After three weeks, the HESS was able to harvest more energy than the conventional system. Figure 13b shows the comparison between these two magnitudes, in the whole design region. The recovery capability has a dependence on the hybridization factor F_{hy} and the autonomy. It can be seen how a higher F_{hy} always means a higher recovery capability, regardless of the value of autonomy. In the selected design region (20% F_{hy}, around 225 h of autonomy), the HESS is able to recover between 1.2 to 1.5 times more energy after low irradiation periods, increasing the reliability of the whole system.

However, there is more variation along the autonomy axis, where three main regions appear. For the lowest and highest autonomy values, the HESS bests the non-hybrid system performance. For medium autonomy values, the improvement is not so evident. In this design zone, the HESS does not suffer blackouts while the conventional ESS does. Thus, the battery of a non-hybrid system, fully discharged, takes longer to reach the float stage and, therefore, it remains in the current stage longer, absorbing more energy. Meanwhile a HESS remains partially charged. This is the reason why the improvement results are not so evident in the medium autonomy region.

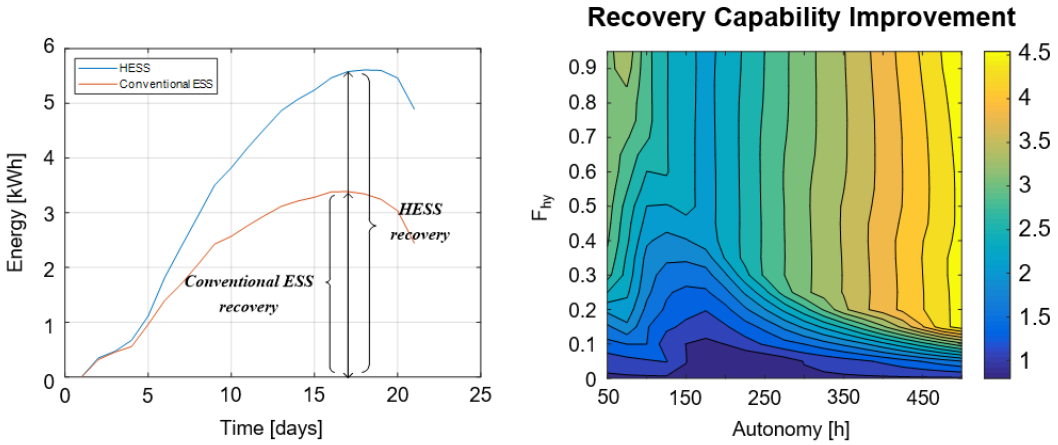

Figure 13. Additional harvested energy in a sample case (**a**), Recovery capability improvement in the design space (**b**).

5. Experimental Results

The HESS concept was tested in the supply system of a metering and communication installation located in an irrigation channel. The connection scheme is the one displayed in Figure 7a. The original supply system was formed by a single VRLA battery pack, four solar panels, and a solar charger. A state of the art bidirectional DC/DC converter, based on EPC-GaN power modules (Figure 14), was designed. The system was tested using $LiFePO_4$ and VRLA batteries with the EMS of Figure 8 as explained in the simulation section. The DC/DC converter is highly efficient and is based on a buck-boost 3-branch interleaved topology [49], but any other DC/DC converter with a reasonable efficiency will lead to almost the same results. The efficiency characteristic of the converter is also shown in the figure. In these first tests, the power through the converter to the $LiFePO_4$ batteries was limited to 200 W.

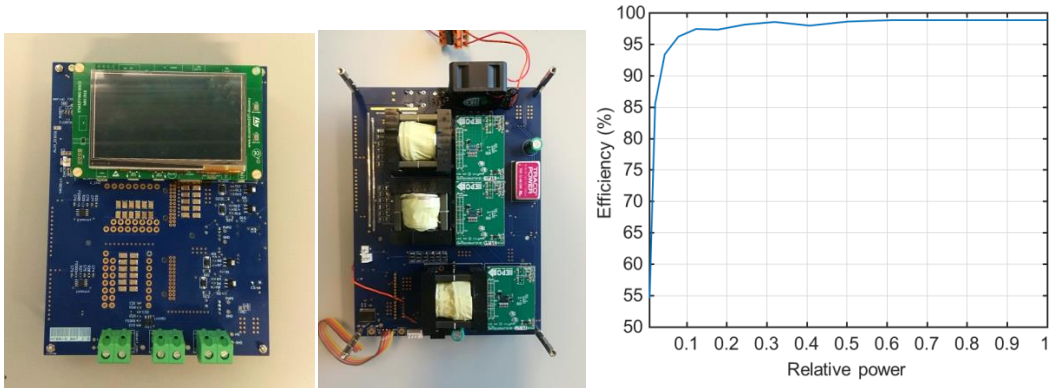

Figure 14. Buck-boost converter front (**left**), Buck-boost converter rear (**center**), measured efficiency of the converter (**right**).

The complete system is shown in Figure 15, with the features shown in Table 2. The energy system presents an autonomy of 144 h and an F_{hy} of 17%. This value for the hybrid factor is close to the optimum in cost efficiency. Additionally, another installation with a simple ESS comprising only the VRLA battery pack is monitored in order to compare absorption and performance results. Both sites are only 2.85 km from each other and therefore operate under the same environmental conditions, such as similar irradiation and temperature. This exact situation was simulated and according to the results, the maximum steady SoE improvement achievable should be around 32%, higher than the non-hybrid case.

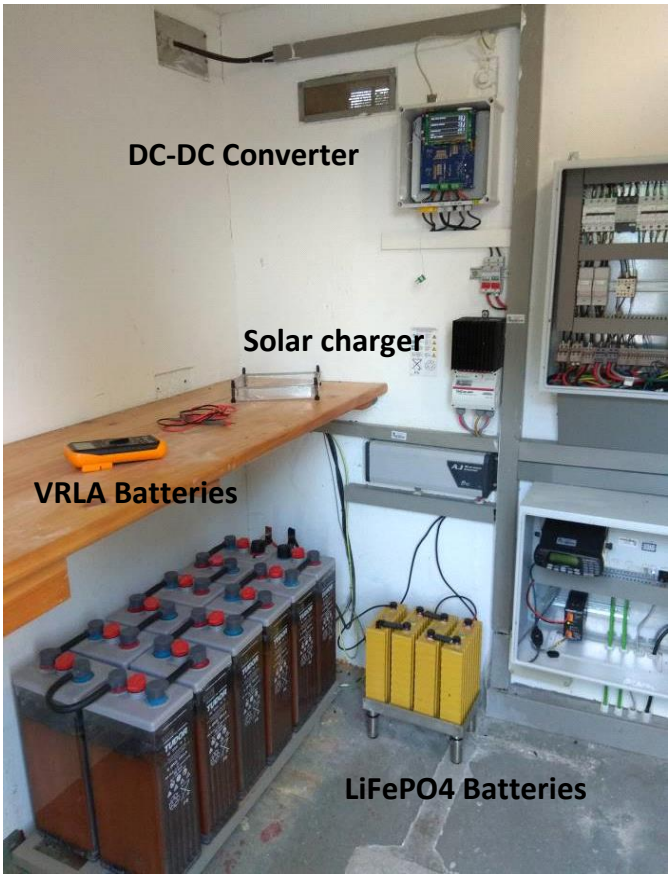

Figure 15. Different elements in the HESS installation.

Table 2. Installation features.

Element	Parameter	Value	Units
VRLA battery	*Cnom*	*420*	*Ah*
	Vnom	*24*	*V*
	Model	*Exide 6 OPzS 420*	-
$LiFePO_4$ battery	*Cnom*	*160*	*Ah*
	Vnom	*12.8*	*V*
	Thunder Sky LYP160AHA(B)		-
Installation	*DC Pcons*	*84*	*W*
	Solar Pgen	*700*	*W*
	Vnom	*24*	*V*
Solar Charger	*Model*	*Morningstar Tristar MPPT TS-45*	-

Results show a good correspondence with simulation. An example of how the system works, featuring typical power patterns in the HESS and in the ESS during autumn days, is shown in Figure 16. After sunrise, power starts coming into the system, and charges the $LiFePO_4$ battery. Right after the 200 W limit is reached, the VRLA battery starts charging.

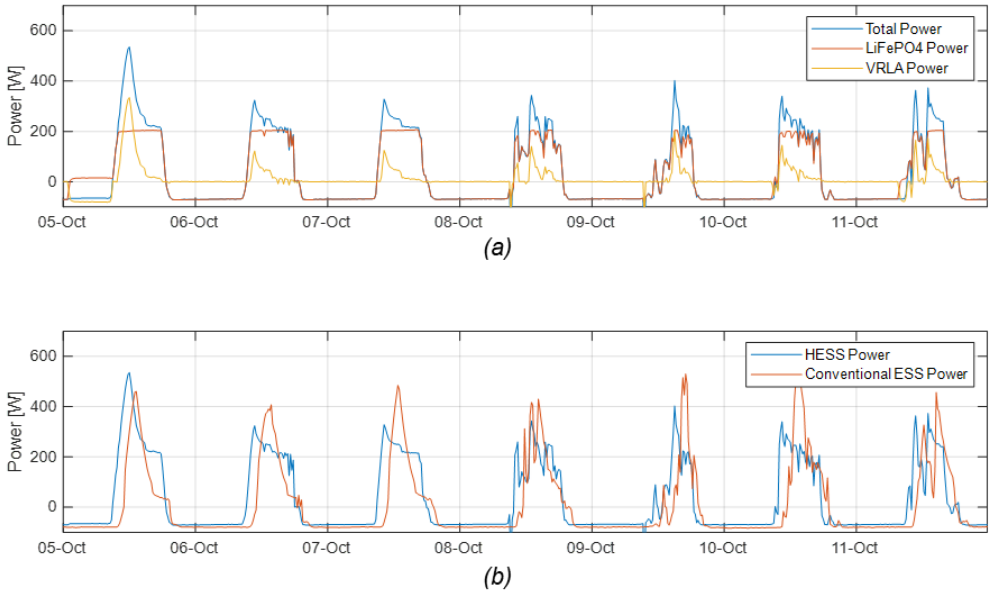

Figure 16. Power flows within the HESS (**a**), Power flows in the HESS and in the Conventional ESS (**b**), October 2018.

When it reaches the float voltage, power starts decreasing, but the $LiFePO_4$ battery continues demanding input power, so the overall generation does not decrease immediately. In Figure 16b, it can be clearly appreciated how the power in the conventional ESS decreases greatly after noon, while in the HESS the $LiFePO_4$ battery is still charging at maximum power, under the same irradiation conditions.

The last figure collates some interesting experimental results obtained during cloudy weeks, in October 2018. As displayed in Figure 17a, the hybrid system is able to harvest an increased amount of energy along the months it was deployed. Specifically, the figure shows three weeks of operation, where the HESS harvested 2 kWh more than the conventional ESS. This means a considerable improvement in the overall efficiency of the installation.

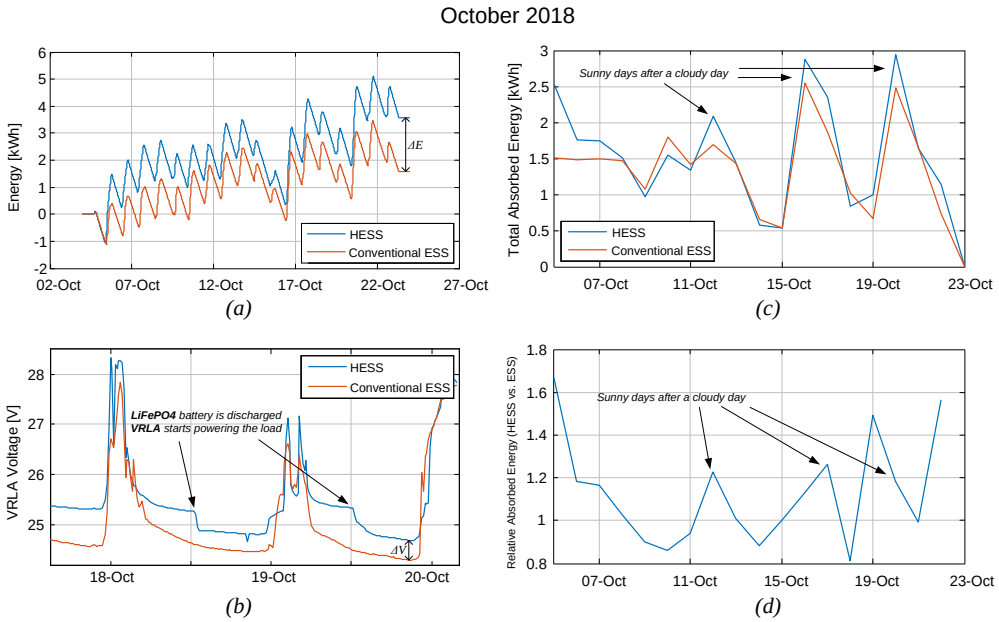

Figure 17. Stored energy (**a**), voltage of VRLA battery (HESS and ESS) (**b**), daily stored energy (HESS and ESS) (**c**), daily absorbed energy (HESS vs. ESS) (**d**).

The increased absorption and the emergency role of the VRLA battery within the HESS makes its steady SoE higher. This is captured in the increase of the VRLA battery voltage; see Figure 17b. The HESS VRLA battery voltage shown in this figure presents a step during the night. This is the moment when the $LiFePO_4$ battery (not plotted) has become fully discharged, and the VRLA battery starts powering the load, in its emergency role. If the voltages are compared at this moment of both VRLA batteries (when there is current flowing through them), a difference of 400 mV (33.3 mV/cell) can be noticed. According to manufacturer this means an energy increase of a 16% [29].

If just the incoming energy in both systems is integrated on a daily basis, the results in Figure 17c are achieved. In them, it can be clearly seen how after low irradiation days, the HESS harvests more energy than the conventional ESS, improving its recovery capability. In Figure 17d, this improvement is established with an increase of 20% of the energy on these specific days.

6. Discussion

PV Off-grid systems suffer from specific generation and consumption profiles that worsen their storage performance when using only one standard battery pack due to PSoC. This study proposes the HESS as a technique to improve this performance, establishing the key sizing parameters. A HESS containing VRLA and $LiFePO_4$ batteries is proposed. The simulation results show a gain from 10% to 40% of the steady-state SoE and an improvement from 20% to 80% of the recovery capabilities after low irradiation days, for HESSs within the optimal design region. A simulation-based analysis leads to an optimum $LiFePO_4$ size between 15% to 30% of the overall installed energy.

A very simple EMS based on priorities was implemented. The EMS is required in order to obtain the first simulation and experimental results, in such a way that the proposed HESS concept is validated. However, there is a huge research field related to new EMSs, leading to strategies that may be better suited to other applications. The EMS was experimentally tested on a real installation with a simple 200 W DC/DC converter. The results show that the proposed HESS concept is able to harvest 20% more energy than the simple ESS. This improvement can be theoretically increased up to a 35% if a higher power DC/DC converter is used.

An interesting result is discussed in the simulation section, where it can be seen how a hybrid $LiFePO_4$–VRLA system with 25% of lithium-based chemistry performs better than a full $LiFePO_4$ system. We can conclude that the split of the battery pack into two packs with different roles has its benefits, and this becomes emphasized if the chemistry of the batteries fits the role. In this case, the $LiFePO_4$ was used as high priority and cyclic storage, while the VRLA was used as emergency storage.

The results of this study are subject to several interpretations. In this application, new HESS do not need to be oversized in order to guarantee a minimum charge reserve when low irradiation days occur. Even more, old ESS based on one monolithic VRLA battery can be retrofitted by adding in parallel the DC/DC converter and the small $LiFePO_4$ battery pack. The old battery can now operate in another regime, as an emergency role, and thus extend its useful life.

Author Contributions: C.B.R., E.O.U. and J.M.C.S. conceptualized and supervised the experiments of the research. C.B.R. and S.J.A.S. contributed to the hardware development. A.B.N. and E.O.U. contributed to the control strategies and system simulation. E.G.P., I.A.L., and J.M.C.S. contributed to the battery modeling and testing. I.S.-G. prepared the original draft and firmware programming. C.B.R., E.O.U., A.B.N., and S.J.A.S. were in charge of the revision and editing of the draft.

Funding: This work was supported in part by the Spanish MINECO under Grant RTC-2015-3358-5 and the LMP_16_18 Grant from the Aragon government RIS3 program.

Acknowledgments: The authors would like to acknowledge the support from Sociedad Ibérica de Construcciones Eléctricas S.A. and from Confederación Hidrográfica del Ebro.

Conflicts of Interest: The authors declare no conflict of interest.

References

1. May, G.J. Recent progress in the development of VRLA batteries for the global telecom market. In Proceedings of the Intelec'96—International Telecommunications Energy Conference, Boston, MA, USA, 6–10 October 1996; IEEE: Piscataway, NJ, USA, 1996; pp. 168–171.
2. Anbuky, A.H.; Pascoe, P.E. VRLA battery state-of-charge estimation in telecommunication power systems. *IEEE Trans. Ind. Electron.* **2000**, *47*, 565–573. [CrossRef]
3. Karthigeyan, V.; Aswin, M.; Priyanka, L.; Sailesh, K.N.D.; Palanisamy, K. A comparative study of lithium ion (LFP) to lead acid (VRLA) battery for use in telecom power system. In Proceedings of the 2017 International Conference on Computation of Power, Energy Information and Commuincation (ICCPEIC), Melmaruvathur, India, 22–23 March 2017; IEEE: Piscataway, NJ, USA, 2017; pp. 742–748.
4. Ragone, D.V. *Review of Battery Systems for Electrically Powered Vehicles*; SAE: Troy, MI, USA, 1968.
5. Christen, T.; Carlen, M.W. Theory of Ragone plots. *J. Power Sources* **2000**, *91*, 210–216. [CrossRef]
6. Oyarbide, E.; Elizondo, I.; Martinez-Iturbe, A.; Bernal, C.; Irisarri, J. Ultracapacitor-based plug & play energy-recovery system for elevator retrofit. In Proceedings of the 2011 IEEE International Symposium on Industrial Electronics, Gdansk, Poland, 27–30 June 2011; IEEE: Piscataway, NJ, USA, 2011; pp. 462–467.
7. Anuphappharadorn, S.; Sukchai, S.; Sirisamphanwong, C.; Ketjoy, N. Comparison the Economic Analysis of the Battery between Lithium-ion and Lead-acid in PV Stand-alone Application. *Energy Procedia* **2014**, *56*, 352–358. [CrossRef]
8. Podder, S.; Khan, M.Z.R. Comparison of lead acid and Li-ion battery in solar home system of Bangladesh. In Proceedings of the 2016 5th International Conference on Informatics, Electronics and Vision (ICIEV), Dhaka, Bangladesh, 13–14 May 2016; IEEE: Piscataway, NJ, USA, 2016; pp. 434–438.
9. Wang, X.; Adelmann, P.; Reindl, T. Use of $LiFePO_4$ Batteries in Stand-Alone Solar System. *Energy Procedia* **2012**, *25*, 135–140. [CrossRef]
10. Jousse, J.; Lemaire, E.; Ginot, N.; Batard, C.; Diouris, J.-F. Assessment of lithium ion $LiFePO_4$ cells usage in photovoltaic standalone systems. In Proceedings of the IECON 2013—39th Annual Conference of the IEEE Industrial Electronics Society, Vienna, Austria, 10–13 November 2013; IEEE: Piscataway, NJ, USA, 2013; pp. 1530–1535.
11. Kim, Y.; Koh, J.; Xie, Q.; Wang, Y.; Chang, N.; Pedram, M. A scalable and flexible hybrid energy storage system design and implementation. *J. Power Sources* **2014**, *255*, 410–422. [CrossRef]
12. Chemali, E.; McCurlie, L.; Howey, B.; Stiene, T.; Rahman, M.M.; Preindl, M.; Ahmed, R.; Emadi, A. Minimizing battery wear in a hybrid energy storage system using a linear quadratic regulator. In Proceedings of the IECON 2015—41st Annual Conference of the IEEE Industrial Electronics Society, Yokohama, Japan, 9–12 November 2015; IEEE: Piscataway, NJ, USA, 2015; pp. 3265–3270.
13. Bocklisch, T. Hybrid Energy Storage Systems for Renewable Energy Applications. *Energy Procedia* **2015**, *73*, 103–111. [CrossRef]
14. Merei, G.; Berger, C.; Sauer, D.U. Optimization of an off-grid hybrid PV–Wind–Diesel system with different battery technologies using genetic algorithm. *Sol. Energy* **2013**, *97*, 460–473. [CrossRef]
15. Rahe, C. Lead-acid Batteries and Lithium-ion Batteries in parallel Strings for an Energy Storage System for a Clinic in Africa. In Proceedings of the 20th International Student Conference on Electrical Engineering, Prague, Czech Republic, 24 May 2016.
16. Lukic, S.M.; Cao, J.; Bansal, R.C.; Rodriguez, F.; Emadi, A. Energy Storage Systems for Automotive Applications. *IEEE Trans. Ind. Electron.* **2008**, *55*, 2258–2267. [CrossRef]
17. Cao, J.; Emadi, A. A New Battery/UltraCapacitor Hybrid Energy Storage System for Electric, Hybrid, and Plug-In Hybrid Electric Vehicles. *IEEE Trans. Power Electron.* **2012**, *27*, 122–132.
18. Cao, J.; Schofield, N.; Emadi, A. Battery balancing methods: A comprehensive review. In Proceedings of the 2008 IEEE Vehicle Power and Propulsion Conference, Harbin, China, 3–5 September 2008; pp. 3–8.
19. Lukic, S.M.; Wirasingha, S.G.; Rodriguez, F.; Cao, J.; Emadi, A. Power Management of an Ultracapacitor/Battery Hybrid Energy Storage System in an HEV. In Proceedings of the 2006 IEEE Vehicle Power and Propulsion Conference, Windsor, UK, 6–8 September 2006; IEEE: Piscataway, NJ, USA, 2006; pp. 1–6.

20. Glavin, M.E.; Hurley, W.G. Ultracapacitor/battery hybrid for solar energy storage. In Proceedings of the 2007 42nd International Universities Power Engineering Conference, Brighton, UK, 4–6 September 2007; IEEE: Piscataway, NJ, USA, 2007; pp. 791–795.
21. Kuperman, A.; Aharon, I. Battery–ultracapacitor hybrids for pulsed current loads: A review. *Renew. Sustain. Energy Rev.* **2011**, *15*, 981–992. [CrossRef]
22. Adelmann, P.; Wolst, O.; Jun He, M.; Hamada, M.; Sengebush, F.; Li, Y.; Kufner, A. Topology and Control Strategy for Hybrid Storage Systems. U.S. Patent US20150270731A1, 24 September 2015.
23. Garayalde, E.; Aizpuru, I.; Canales, J.M.; Sanz, I.; Bernal, C.; Oyarbide, E. Análisis Experimental del Efecto de la Temperatura y la Tensión de Carga para la Optimización Energética de Sistemas de Almacenamiento de Instalaciones Fotovoltaicas Aisladas. In Proceeding of the SAAEI, Valencia, Spain, 5–7 July 2017.
24. Sanz-Gorrachategui, I.; Bernal, C.; Oyarbide, E.; Garayalde, E.; Aizpuru, I.; Canales, J.M.; Bono-Nuez, A. New battery model considering thermal transport and partial charge stationary effects in photovoltaic off-grid applications. *J. Power Sources* **2018**, *378*, 311–321. [CrossRef]
25. Swingler, A.; Colgate, G. 12 Years of Residential 'Off-Grid' PV Hybrid System Operation and Evolution in Nemiah Valley, Canada. In Proceedings of the 3rd International Hybrid Power Systems Workshop, Tenerife, Spain, 8–9 May 2018.
26. Swingler, A.; Torrealba, J. Opportunity for Improving Lead-Acid Battery Management of Photovoltaic-Genset-Battery Hybrid Power Systems Based on Measured Field Data. *Energies* **2019**, *12*, 2237. [CrossRef]
27. Moseley, P.T.; Rand, D.A. Partial State-of-Charge Duty: A Challenge but Not a Show-Stopper for Lead-Acid Batteries! *ECS Trans.* **2012**, *41*, 3–16.
28. Jing, W.; Lai, C.H.; Ling, D.K.X.; Wong, W.S.H.; Wong, M.L.D. Battery lifetime enhancement via smart hybrid energy storage plug-in module in standalone photovoltaic power system. *J. Energy Storage* **2019**, *21*, 586–598. [CrossRef]
29. GNB Industrial Power. *Exide Technologies Handbook for Stationary Vented Lead-Acid Batteries Part 2: Installation, Commissioning and Operation*; GNB Industrial Power: Büdingen, Germany, 2012; pp. 1–68.
30. Albright, G.; Edie, J.; Al-Hallaj, S. *A Comparison of Lead Acid to Lithium-ion in Stationary Storage Applications*; AllCell Technologies LLC: Chicago, IL, USA, 2012; p. 14.
31. Liu, J.; Gao, D.; Cao, J. Study on the effects of temperature on $LiFePO_4$ battery life. In Proceedings of the 2012 IEEE Vehicle Power and Propulsion Conference, Seoul, Korea, 9–12 October 2012; IEEE: Piscataway, NJ, USA, 2012; pp. 1436–1440.
32. Krieger, E.M.; Cannarella, J.; Arnold, C.B. A comparison of lead-acid and lithium-based battery behavior and capacity fade in off-grid renewable charging applications. *Energy* **2013**, *60*, 492–500. [CrossRef]
33. Khatib, T.; Ibrahim, I.A.; Mohamed, A. A review on sizing methodologies of photovoltaic array and storage battery in a standalone photovoltaic system. *Energy Convers. Manag.* **2016**, *120*, 430–448. [CrossRef]
34. Kebaïli, S.; Benalla, H. Optimal sizing of a stand-alone photovoltaic systems under various weather conditions in Algeria. *Rev. Energies Renouvelab.* **2015**, *18*, 179–191.
35. Shen, W.X. Optimally sizing of solar array and battery in a standalone photovoltaic system in Malaysia. *Renew. Energy* **2009**, *34*, 348–352. [CrossRef]
36. Jing, W.; Lai, C.H.; Wong, W.S.H.; Wong, M.L.D. A comprehensive study of battery-supercapacitor hybrid energy storage system for standalone PV power system in rural electrification. *Appl. Energy* **2018**, *224*, 340–356. [CrossRef]
37. Kutkut, N.H.; Divan, D.M. Dynamic equalization techniques for series battery stacks. In Proceedings of the Proceedings of Intelec'96—International Telecommunications Energy Conference, Boston, MA, USA, 6–10 October 1996; IEEE: Piscataway, NJ, USA, 1996; pp. 514–521.
38. Ceraolo, M. New dynamical models of lead-acid batteries. *IEEE Trans. Power Syst.* **2000**, *15*, 1184–1190. [CrossRef]
39. Barsali, S.; Ceraolo, M. Dynamical Models of Lead-Acid Batteries: Implementation Issues. *IEEE Trans. Energy Convers.* **2002**, *17*, 16–23. [CrossRef]
40. Pascoe, P.E.; Anbuky, A.H. VRLA battery discharge reserve time estimation. *IEEE Trans. Power Electron.* **2004**, *19*, 1515–1522. [CrossRef]
41. Chen, M.; Rincon-Mora, G.A. Accurate Electrical Battery Model Capable of Predicting Runtime and I–V Performance. *IEEE Trans. Energy Convers.* **2006**, *21*, 504–511. [CrossRef]

42. Coleman, M.; Hurley, W.G.; Chin Kwan Lee, C.K. An Improved Battery Characterization Method Using a Two-Pulse Load Test. *IEEE Trans. Energy Convers.* **2008**, *23*, 708–713. [CrossRef]
43. Coleman, M.; Lee, C.K.; Zhu, C.; Hurley, W.G. State-of-charge determination from EMF voltage estimation: Using impedance, terminal voltage, and current for lead-acid and lithium-ion batteries. *IEEE Trans. Ind. Electron.* **2007**, *54*, 2550–2557. [CrossRef]
44. Günther, M.; Feldmann, U.; ter Maten, J. Modelling and Discretization of Circuit Problems. *Handb. Numer. Anal.* **2005**, *13*, 523–659.
45. Macdonald, J.R.; Brachman, M.K. The Charging and Discharging of Nonlinear Capacitors. *Proc. IRE* **1955**, *43*, 71–78. [CrossRef]
46. Wyatt, J.L. *Foundations of Nonlinear Network Theory*; University of California: Berkeley, CA, USA, 1978.
47. Muthuswamy, B.; Banerjee, S. *Introduction to Nonlinear Circuits and Networks*; Springer: Berkeley, CA, USA, 2018.
48. Ansean, D.; Garcia, V.M.; Gonzalez, M.; Blanco-Viejo, C.; Viera, J.C.; Pulido, Y.F.; Sanchez, L. Lithium-Ion Battery Degradation Indicators Via Incremental Capacity Analysis. *IEEE Trans. Ind. Appl.* **2019**, *55*, 2992–3002. [CrossRef]
49. Garcia, O.; Zumel, P.; de Castro, A.; Cobos, A. Automotive DC-DC bidirectional converter made with many interleaved buck stages. *IEEE Trans. Power Electron.* **2006**, *21*, 578–586. [CrossRef]